Paradoxical Effects of Substitution and Deletion Mutation of Arg56 on the Structure and Chaperone Function of Human αB-Crystallin †

ARTICLE *in* BIOCHEMISTRY · MARCH 2007

Impact Factor: 3.02 · DOI: 10.1021/bi061323w · Source: PubMed

7 AUTHORS, INCLUDING:

Ashis Biswas
Indian Institute of Technology Bhubaneswar
35 PUBLICATIONS **430** CITATIONS

SEE PROFILE

Santhoshkumar Puttur
University of Missouri
42 PUBLICATIONS **728** CITATIONS

SEE PROFILE

BIOCHEMISTRY

 Volume 46, Number 5 February 6, 2007

Articles

Paradoxical Effects of Substitution and Deletion Mutation of Arg56 on the Structure and Chaperone Function of Human αB-Crystallin†

Ashis Biswas,‡ Jeffery Goshe,‡ Antonia Miller,‡ Puttur Santhoshkumar,§ Carol Luckey,|| Manjunatha B. Bhat,⊥ and Ram H. Nagaraj*,‡,#

Departments of Ophthalmology and Pharmacology, and the Visual Sciences Research Center, Case Western Reserve University, Cleveland, Ohio 44106, Center for Anesthesiology Research, Cleveland Clinic, Cleveland, Ohio 44195, and Mason Eye Institute, University of Missouri, Columbia, Missouri 65212

Received June 30, 2006; Revised Manuscript Received October 16, 2006

ABSTRACT: Human αB-crystallin is a small heat-shock protein that functions as a molecular chaperone. Recent studies indicate that deletion of a peptide ($_{54}$FLRAPSWF$_{61}$) from its N-terminus makes it a better chaperone, and this particular sequence is thought to participate in substrate interaction and subunit exchange with αA-crystallin. To determine whether the positive charge on arginine 56 (R56) influences these functions, we prepared human αB-crystallin mutants in which R56 was deleted (ΔR56) or replaced by alanine (R56A). To determine if the effects are specific to R56, we generated two additional mutant proteins in which the two neighboring amino acids were deleted (ΔL55 and ΔA57). Dynamic light scattering studies suggested that none of the mutations affected the oligomeric mass of the protein. Far-ultraviolet circular dichroism (UV CD) spectra revealed greater helicity in the secondary structures of R56A and ΔR56 compared to that of the wild-type (Wt) protein. Near-UV CD spectra showed that the tertiary structure is perturbed in all mutants. Insulin and citrate synthase aggregation assays showed 38 and 30% improvement of chaperone function in ΔR56 compared to that of the Wt. In contrast, the R56A mutant lost most of its chaperone function. Deletion mutants, ΔL55 and ΔA57, showed no significant changes in the chaperone function compared to that of the Wt. The ΔR56 mutant had a higher surface hydrophobicity than the Wt, but the R56A mutant had a lower hydrophobicity. Our data show paradoxical effects of the deletion and substitution of R56 and imply that the chaperone function of human αB-crystallin is dictated not only by the positive charge on R56 but also by the conformational change that it bestows on the protein.

The term "crystallin" refers to a group of soluble structural proteins in the mammalian lens responsible for its refractive properties. The principal component of the lens is α-crystallin, a protein whose abundance varies between species (*1*, *2*). The other protein components of the lens are *β*- and *γ*-crystallin (*3*−*5*). These proteins, combined within the lens of the eye, form an extremely dense mass, ranging in concentration from 300 to 450 mg/mL (*6*, *7*). This protein-rich tissue is not only transparent but also provides mechanical and structural stability to the lens. α-Crystallin has two subunits, αA and αB, that share 60% sequence homology. These subunits belong to the superfamily of small heat-shock proteins (sHSPs)[1] (*8*−*11*). The two subunits, with a monomeric size of 20 kDa, usually associate to form large oligomers of approximately 800 kDa in molecular weight.

† This study was supported by NIH Grants R01EY-016219 and R01EY-09912 (to R.H.N.), P30EY-11373 (Visual Sciences Research Center of Case Western Reserve University), Research to Prevent Blindness (RPB), NY and Ohio Lions Eye Research Foundation.

* To whom correspondence should be addressed: Department of Ophthalmology, Case Western Reserve University, Wearn Building, Room 653, Cleveland, OH 44106. Telephone: 216-844-1132. Fax: 216-844-7962. E-mail: ram.nagaraj@case.edu.

‡ Department of Ophthalmology, Case Western Reserve University.

§ University of Missouri.

|| Visual Sciences Research Center, Case Western Reserve University.

⊥ Cleveland Clinic.

Department of Pharmacology, Case Western Reserve University.

10.1021/bi061323w CCC: $37.00
Published on Web 01/12/2007

Recent studies revealed αB-crystallin in various other tissues besides the lens, including the heart, lung, skeletal muscle, kidney, and brain (*12*−*14*). The lens has the highest concentration of αA-crystallin, although small amounts have been detected in the spleen and thymus as well (*15*).

Horwitz reported in 1992 that α-crystallin functions as a molecular chaperone in the lens, where it prevents the aggregation of thermally or chemically denatured proteins (*16*). It is now believed that this function is essential for maintaining lens transparency during aging. Homology-modeling studies of α-crystallin and a sequence comparison between several sHSPs show that a sequence of 80−100 amino acids is evolutionarily conserved; this sequence is commonly referred to as the "α-crystallin domain" (*17*−*19*). It is flanked by a N- and C-terminal domain (generally designated as the C-terminal extension). The unstructured C-terminal region contains a large number of charged residues, which are believed to aid in the solubilization of α-crystallin (*20*). Several studies suggest that this unstructured C-terminal region could also significantly influence the structure, chaperone-like activity, and subunit interaction of the protein (*21*−*25*). However, other studies assign the N-terminal region a critical role in oligomerization and chaperone function (*26*, *27*). Additional papers identified specific residues or sequences in each domain as important for the complex assembly and chaperone activity of αA- and αB-crystallin (*27*−*30*).

Mutation analysis studies established that arginine residues at different positions influence oligomerization, chaperone function, and subunit interaction of α-crystallin (*31*−*37*). Sharma and co-workers recently reported that deletion of $_{54}$FLRAPSWF$_{61}$ from the N-terminal domain of human αB-crystallin improves its chaperone function (*38*). Ghosh et al. (*30*) found that the $_{43}$SLSPFYLRPPSFLRAP$_{58}$ sequence in αB-crystallin is the substrate interaction site during chaperone function and a site for subunit interaction with αA-crystallin. We believe that arginine at position 56 within this sequence is important for both chaperone function and subunit interaction. This is based on our previous studies on αA-crystallin that showed that R21 and R103 are important regulators of chaperone function (*37*, *39*). Therefore, to better understand the role of arginine 56, we used site-directed mutagenesis to prepare two kinds of αB-crystallin mutants: a deletion mutant (ΔR56) and a substitution mutant (R56A). To establish the specificity for R56, we prepared two additional mutants where the amino acids adjacent to R56 (leucine 55 and alanine 57) were deleted (ΔL55 and ΔA57). We report our findings on the structure, function, and biophysical characteristics of these proteins and describe the contrasting effects of substitution and deletion mutation of R56 in αB-crystallin.

EXPERIMENTAL PROCEDURES

Materials. Bovine insulin, citrate synthase (CS), and dithiothreitol (DTT) were obtained from Sigma Chemical Co., St. Louis, MO. CS was dialyzed for 24 h against 40 mM *N*-2-hydroxyethylpiperazine-*N*′-2-ethanesulfonic acid (HEPES) buffer (pH 7.4) before use. 2-(*p*-Toludino)naphthalene-6-sulfonic acid (TNS), Alexa fluor 350, and Alexa fluor 488 were obtained from Molecular Probes (Invitrogen, Carlsbad, CA). All other chemicals were of analytical grade.

Cloning and Site-Directed Mutagenesis. The cDNA encoding the human αB-crystallin was kindly provided by J. Mark Petrash, Washington University, St. Louis, MO. The wild-type (Wt) and mutant (ΔL55, ΔR56, ΔA57, and R56A) αB-crystallin cDNAs were generated by polymerase chain reaction (PCR) amplification and cloned into the prokaryotic expression vector pET-23(d+) (Novagen, Madison, WI) using restriction sites *Nco* I (5′) and *Hin*d III (3′). Mutations were introduced using the megaprimer PCR approach. The following primers were used as described: Wt, forward (P1), 5′-CATGCCATGGGGCACCACCACCACCACCACATGGACATCGCCATCCACCAC-3′; Wt, reverse (P2), 5′-CCCAAGCTTCTATTTCTTGGGGGCTGCGGT-3′; ΔR56, reverse (P3), 5′-AAACCAGCTGGGTGCCAGGAAGGAGGGTGG-3′; R56A, reverse (P4), 5′-CCAGCTGGGTGCCGCCAGGAAGGAGGG-3′; ΔL55, reverse (P5), 5′-CCAGCTGGGTGCCCGGAAGGAGGGTGGCCG-3′; and ΔA57, reverse (P6), 5′-GTCAAACCAGCTGGGCCGCAGGAAGGAGGG-3′. The P1 primer contains the sequence encoding six histidine residues, which are added on the N-terminal end. This helps to purify the expressed protein with a Ni−nitrilotriacetic acid (NTA) resin as described below. The cDNA encoding the full-length αB-crystallin was used as the template in all PCR amplifications with Pfu turbo DNA polymerase (Stratagene, La Jolla, CA). We obtained His-tagged cDNA encoding the full-length αB-crystallin with the P1 and P2 primer pair. Mutant cDNAs were generated as follows: the PCR product obtained from the primer combination of P1 and P3 was used as a megaprimer along with the reverse primer P2 in the subsequent PCR reaction. This enabled us to obtain the αB-crystallin bearing the ΔR56 mutantion. Other mutants were obtained in the same way, where the PCR products obtained from the combination of primers P1 and P4, P1 and P5, or P1 and P6 were used as the megaprimers along with the primer P2 to obtain the R56A, ΔL55, and ΔA57 mutant cDNAs, respectively. The Wt and mutant cDNAs were then cloned into the pET-23-(d+) vector, and mutations were confirmed by DNA sequencing and further confirmed by determination of the molecular weight by electrospray ionization (ESI)−mass spectrometry.

Protein Expression and Purification. Escherichia coli BL21(DE3)pLysS were transformed with pET-23(d+) plasmids containing either the Wt or mutant αB-crystallin cDNA. Proteins were expressed and purified as follows: 500 mL of LB medium supplemented with ampicillin (100 μg/mL) was inoculated with 50 mL of an overnight bacterial culture and cultured at 37 °C and 250 rpm until the optical density (OD at 600 nm) was 0.5−0.7. Induction of αB-crystallin expression was initiated by the addition of 250 μM isopropyl-β-D-thiogalactoside (IPTG). The cultures were then grown for an additional 4−5 h at 37 °C, and the cells were harvested by centrifugation at 5000*g* for 10 min at 4 °C. The cell pellets were resuspended at 5 g/mL of lysis buffer (100 mM NaH_2PO_4, 10 mM Tris, and 8 M urea at pH 8) and gently mixed for 1 h at room temperature. Lysates were immersed in ice and dispersed by sonication (3 × 40 s bursts at 40% amplitude) with a Branson Digital Sonifier (Danbury, CT).

[1] Abbreviations: sHSP, small heat-shock protein; DTT, dithiothreitol; IPTG, isopropyl-β-D-thiogalactoside; CS, citrate synthase; TNS, 2-(*p*-toludino)naphthalene-6-sulfonic acid, sodium salt; FRET, fluorescence resonance energy transfer.

All samples were centrifuged at 12000*g* for 30 min. With the supernant and pellet fractions, we performed sodium dodecyl sulfate−polyacrylamide gel electrophoresis (SDS−PAGE) and found that both the Wt and mutant proteins were present mostly in the supernatant fractions (data not shown). Each lysate was then incubated with the appropriate amount of Ni−NTA resin according to the instructions of the manufacturer (Qiagen, Valencia, CA) and gently mixed for 1 h at room temperature before loading onto a prepared column. The columns were washed with buffer (pH 7.0) containing 100 mM NaH_2PO_4, 10 mM Tris, and 8 M urea and eluted with the same buffer at pH 5.5. The eluted proteins were separated by SDS−PAGE, and immunoreactivity was assessed by Western blotting with an antibody to αB-crystallin (see below). Proteins that appeared as a single band at 20 kDa were pooled and dialyzed extensively at 4 °C against 50 mM Tris-HCl (pH 8.0). The pooled protein was then concentrated using Amicon Ultra-15 centrifugal filters (Millipore) and stored at −20 °C. The yield for all proteins was ∼15−20 mg/L of culture.

SDS−PAGE and Western Blotting. Mutant and Wt proteins (1 μg) and protein standards (Precision Protein Standard, Bio-Rad Laboratories, Hercules, CA) were loaded onto two 12% SDS−PAGE gels and subjected to electrophoresis at 150 V for 1.5 h. After this time, one gel was stained with Bio-Safe Coomassie (Bio-Rad), and the protein from the other was transferred electrophoretically to a nitrocellulose membrane (100 V for 1 h). The membrane was blocked by overnight incubation at 4 °C in buffer A [5% NFDM in phosphate-buffered saline (PBS)]. The blocked membrane was then incubated with monoclonal mouse anti-αB-crystallin antibody (1:1000) (Stressgen, Victoria, British Columbia, Canada) in buffer A at room temperature for 1 h. After this initial incubation, the membrane was washed extensively with 0.05% Tween-20 in PBS and incubated for 1 h at room temperature with a 1:3000 dilution of horseradish peroxidase (HRP)-conjugated goat antimouse-IgG (Sigma) in 0.05% Tween-20 in PBS. The membrane was washed again with 0.05% Tween-20, developed with SuperSignal West Pico Chemiluminescent stain (Pierce, Rockford, IL), and photographed.

Molecular-Size Determination. The molecular size of the Wt and mutant proteins was determined by dynamic light scattering measurements as described earlier (*40*). Briefly, the Wt and mutant proteins were incubated at 37 °C for 1 h and then chromatographed on a TSK G5000PW_{XL} (Tosoh Bioscience, Inc., San Francisco, CA) size-exclusion column using 50 mM phosphate buffer containing 0.3 M NaCl (pH 7.2). The size-exclusion column was connected to a high-performance liquid chromatograph (HPLC) equipped with a refractive index detector (Shimadzu) and coupled to multi-angle light scattering (DAWN) and quasi-elastic light scattering detectors (Wyatt Technology Corp., Santa Barbara, CA). The molar mass (M_w), polydispersity index (PDI), and hydrodynamic radius (R_h) of the proteins were determined with ASTRA (5.1.5) software (Wyatt Technology Corp.).

Tryptophan Fluorescence Measurements. Wt and mutant αB-crystallins (0.l mg/mL) were prepared in 50 mM phosphate buffer (pH 7.2). Fluorescence emission spectra of these samples were recorded between 310 and 400 nm by a LS-55 Perkin Elmer spectrofluorometer at 25 °C with an excitation and emission band pass of 5 nm. The tryptophan emission was measured following excitation at 295 nm. Data were collected at 0.5 nm wavelength resolution.

Circular Dichroism (CD) Measurements. Changes in secondary and tertiary protein structure were measured by far- and near-ultraviolet (UV) CD spectra at 25 °C in a Jasco 810 spectropolarimeter (Jasco, Inc., Japan). Far-UV measurements were made with 0.2 mg/mL proteins in 10 mM phosphate buffer (pH 7.2); near-UV measurements were measured with 1 mg/mL protein in the same buffer. Far- and near-UV CD spectra were recorded in CD quartz cells of 1 or 10 mm path length. An average of spectra over five scans was analyzed for secondary structure by the curve-fitting program CONTINLL (*41*).

Determination of Structural Stability. The structural stability of Wt and mutant αB-crystallins was determined by equilibrium chemical denaturation experiments. A solution of α-crystallin (0.1 mg/mL in 50 mM phosphate buffer at pH 7.2) was incubated for 18 h at 25 °C with various concentrations of urea (0−7 M). Tryptophan fluorescence spectra were acquired in the 310−400 nm region for all protein solutions using 295 nm as the excitation wavelength and 5 nm each for excitation and emission band passes. The equilibrium unfolding profile was then fitted according to a three-state model as described in ref *42*.

TNS Fluorescence Measurements. The surface hydrophobicity of Wt and mutant human αB-crystallins was measured with a specific hydrophobic probe, TNS. A methanolic solution of TNS (100 μM) was added to a 0.1 mg/mL protein solution in 50 mM phosphate buffer (pH 7.4), and the mixture was incubated for 2 h at 25 °C. The protein samples were excited at 320 nm, and fluorescence emission spectra were recorded between 350 and 520 nm. The excitation and emission band passes were 5 nm each.

Chaperone Function of Wt and Mutant Human αB-Crystallins. The chaperone function was determined using insulin and CS as substrate proteins. Both assays were done in 96-microwell plates in a microplate reader (Molecular Devices, SpectraMax, Model 190, Sunnyvale, CA). The total volume of the reaction mixture was 250 μL.

(*a) Insulin Aggregation Assay.* Insulin (80 μg) in 50 mM phosphate buffer (pH 7.2) was incubated at 25 °C in the presence and absence of Wt or mutant αB-crystallin (16 μg). The reduction of insulin was initiated with 20 mM DTT, and the extent of insulin B chain aggregation was measured by monitoring light scattering at 360 nm for 1 h (*43*).

(*b) CS Aggregation Assay.* CS (15 μg) in 40 mM HEPES buffer (pH 7.4) was heated at 43 °C with and without the different αB-crystallin preparations (5 μg), and light scattering was monitored at 360 nm for 1 h (*44*). Both assays were carried out at different ratios of αB-crystallins and substrate proteins.

Estimation of Binding Parameters between αB-Crystallin and Carbonic Anhydrase (CA). We incubated 12.5 μM Wt or mutant αB-crystallin with 2−18 μM CA for 1 h at 57 °C in 50 mM phosphate buffer containing 100 mM NaCl (pH 7.2). We observed no protein aggregation under these conditions. The solutions were cooled to 25 °C for 1 h. Unbound substrate was then separated from the "αB-crystallin−CA complex" by centrifugation at 4000*g* through 100 kDa cut-off membrane filters. The amount of substrate (CA) bound by αB-crystallin was calculated by subtracting free substrate from the total substrate concentration. We

determined unbound substrate protein, i.e., CA, concentrations by two different methods, one by measuring the absorbance at 280 nm and using an extinction coefficient of 1.9 (mg/mL protein)$^{-1}$ cm^{-1} for CA and the other by the Bradford assay. The magnitude of the unbound substrate concentration obtained with the spectroscopic method was almost similar to what we obtained with the Bradford assay method. The number of binding sites (n) and dissociation constant (K_d) were determined by a similar procedure (*45*).

Fluorescence Labeling of Recombinant αA-, αB-, and αB-Crystallin Mutants with Alexa Fluor 488 and Alexa Fluor 350. Purified recombinant αA-crystallin was conjugated with Alexa fluor 488, and Wt αB and its mutants were conjugated with Alexa fluor 350 fluorescent probes as described by the manufacturer (Molecular Probes, Invitrogen, Carlsbad, CA). Briefly, protein samples (1 mg/mL) in 50 mM PBS supplemented with 100 mM sodium bicarbonate (pH 7.2) were mixed with Alexa fluor probes for 1 h at 25 °C. The covalently labeled α-crystallins were separated by passage through BioGel P-30 columns equilibrated with PBS (pH 7.2). The first fluorescent peak, which contained the labeled protein, was collected and dialyzed against 50 mM PBS (pH 7.2) for 24 h. The amount of αA-crystallin labeled with Alexa fluor 488 was calculated by measuring the absorbance at 280 and 494 nm of αA-crystallin and Alexa fluor 488, respectively. The percentage of fluorescence labeling of Alexa fluor 350 to Wt and mutant αB-crystallins was calculated from the absorbance of αB-crystallin and Alexa fluor 350 at 280 and 346 nm, respectively. Concentrations of Alexa fluor 488 and Alexa fluor 350 were determined from their absorption spectra using molar extinction coefficients of 71 000 cm^{-1} M^{-1} at 494 nm and 19 000 cm^{-1} M^{-1} at 346 nm, respectively.

Measurements of the Subunit Exchange Rate. We noted a significant overlap of the emission spectrum of the Alexa Fluor 350 fluorophore with the absorption spectrum of the Alexa Fluor 488 fluorophore. The excitation maxima of Alexa fluor 350-labeled αB-crystallin was 346 nm, with an emission maximum of 440 nm. The Alexa fluor 488-labeled αA-crystallin had an excitation maximum of 494 nm and an emission maximum of 520 nm. This overlap indicates that these two flurophores are an excellent donor−acceptor pair for fluorescence resonance energy transfer (FRET). We measured subunit exchange kinetics according to Sreelakshmi et al. (*28*). Subunit exchange experiments combined 25 μg of Alexa fluor 350-labeled Wt or mutant αB-crystallins as energy donors (each separately) with 75 μg of Alexa fluor 488-labeled αA-crystallin as the energy acceptor. The proteins were incubated for 2 h at 37 °C in PBS (pH 7.2) in a ratio of 3:1 αA/αB to mimic the conditions *in vivo*. At different time intervals, fluorescence spectra (400−600 nm) of the various samples were taken at the same temperature using a Fluoromax-2 (Jobin Yvon Spex, Horiba Group) spectrofluorometer. The excitation wavelength was 346 nm. The band pass of both excitation and emission monochromators was 5 nm each. We determined the intensity at 440 nm and calculated the subunit exchange rate from this equation

$$F(t)/F(0) = A + Be^{-kt} \quad (1)$$

where $F(t)$ is the fluorescence intensity at 440 nm at different time intervals, $F(0)$ is the fluorescence intensity at 440 nm at $t = 0$, and k is the subunit exchange rate constant. Constants A and B were determined using conditions where $A + B = 1$ at $t = 0$ and A is the fluorescence intensity at $t = \infty$. We then determined the rate constant by nonlinear regression analysis of the data with Origin 6.0 software.

RESULTS AND DISCUSSION

Previous studies indicated that deletion of the first 63 N-terminal residues from αA-crystallin drastically reduces its oligomeric size (from 800 to 60 kDa), but this deletion has no effect on subunit exchange (*26*). Peptide scans established the requirement for residues 42−57 and 60−71 of αB-crystallin for the interaction with αA-crystallin (*28*). A recent study by Santhoshkumar and Sharma revealed that deletion of amino acid residues 54−61 from the N-terminal domain of αB-crystallin improves its chaperone function (*38*). Soon after this discovery, another study confirmed the role of residues 43−57 in human αB-crystallin in chaperone activity and showed that this sequence was also involved in subunit assembly (*30*). Thus, it appears that the peptide $_{43}$-SLSPFYLRPPSFLRAPSWF$_{61}$ is critical for protein oligomerization, chaperone function, and subunit interaction in αB-crystallin.

Previous studies have established that arginine residues strongly influence the structure, function, and subunit interaction in both αA- and αB-crystallins (*31*−*37*, *39*). There are two arginine residues between residues 43 and 61 in αB-crystallin, one at the 50th position and another at the 56th position. Because R50 affects neither the structure nor chaperone function (*28*), we explored how R56 in αB-crystallin influenced its structure, chaperone function, and subunit interactions with αA-crystallin. Findings from our earlier study (*39*) suggested that the enhancement of the chaperone function by deletion of $_{54}$FLRAPSWF$_{61}$ (*38*) might be due to the removal of the positive charge on R56. Accordingly, we undertook a detailed study to determine exactly how this residue affects the structure and chaperone function of αB-crystallin.

To differentiate specific effects as a result of R56 from nonspecific effects that could result from amino acid mutation, we generated several mutant proteins, including those in which R56 was either deleted (ΔR56) or substituted with alanine (R56A) and proteins in which amino acids adjacent to R56 are deleted (ΔL55 and ΔA57). We cloned and expressed hexa-His-tagged Wt and mutant αB-crystallins in *E. coli* BL21(DE3)pLysS cells and then purified the proteins. After the proteins passed through a Ni column, we checked the purity of the proteins by SDS−PAGE and Western blotting (with a monoclonal antibody to αB-crystallin). These procedures identified a single band in all samples, including those with selected mutations as well as the Wt (Figure 1). The molecular weight was determined by ESI−mass spectrometry and was as follows (including six histidines plus one glycine): 21 038 Da for Wt, 20 925 Da for ΔL55, 20 882 Da for ΔR56, 20 907 Da for ΔA57, and 20 953 Da for R56A and were fully compatible with the expected molecular weight of proteins.

To define the role of R56 in the chaperone function, we first used two target proteins, insulin and CS, to examine how ΔL55, ΔR56, ΔA57, and R56A influenced chaperone

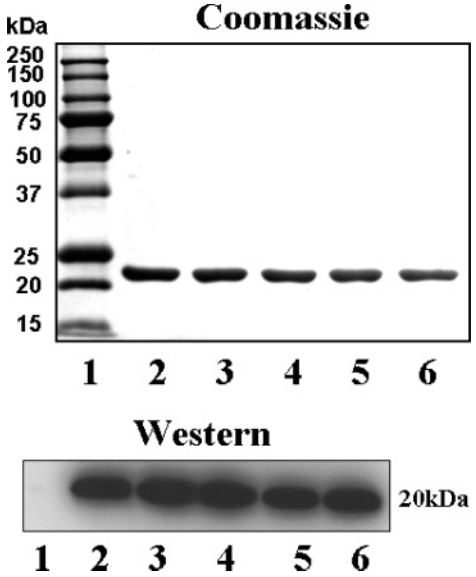

FIGURE 1: Purification of human recombinant αB-crystallin. A total of 1 μg of purified protein was subjected to SDS−PAGE on a 12% reducing gel and then either stained with Coomassie blue or Western blotted using a mouse monoclonal antibody to human αB-crystallin. Lane 1, molecular-weight markers; lane 2, Wt; lane 3, ΔL55; lane 4, ΔR56; lane 5, ΔA57; and lane 6, R56A.

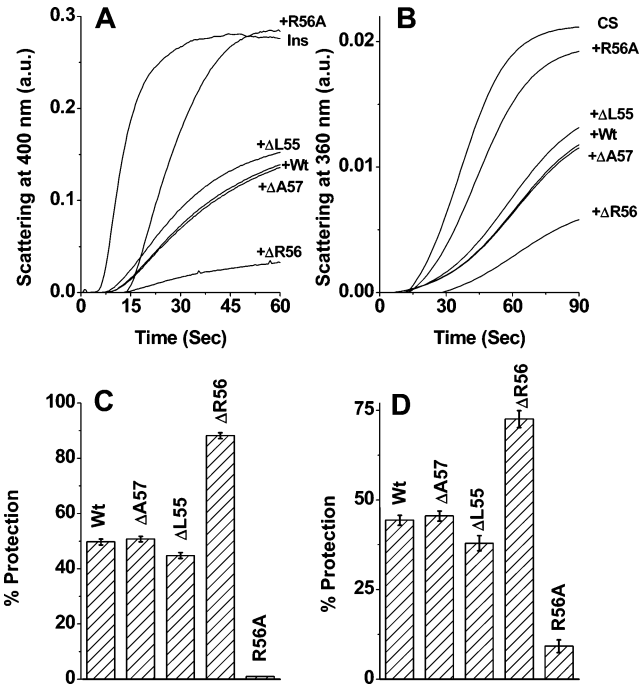

FIGURE 2: Chaperone function of human αB-crystallin. (A and B) DTT-induced aggregation of 0.32 mg/mL insulin at 25 °C and thermal aggregation of 0.06 mg/mL CS at 43 °C with and without αB-crystallins. The chaperone/substrate ratio (w/w) was 1:5 and 1:3 for insulin and CS aggregation assays, respectively. The percent protection ability of different αB-crystallins against insulin (C) and CS aggregation (D). Data are means ± standard deviation from triplicate determinations.

function. Figure 2A shows the profile of DTT-induced aggregation of insulin in the presence or absence of Wt and mutant αB-crystallins. At a ratio of 1:5 (w/w) of Wt/insulin, we noted ∼50% protection against aggregation (Figure 2C). Remarkably, under the same conditions, ΔR56 increased chaperone function further to provide ∼88% protection (Figure 2C). In contrast, the R56A mutant completely failed to prevent insulin aggregation (Figure 2C). The two other mutations, ΔL55 and ΔA57, had no effect on chaperone function, and the extent of inhibition of insulin aggregation was comparable to that of the Wt.

We used analysis of CS aggregation as another means of measuring chaperone function. Thermal aggregation of this protein occurs upon incubation at 43 °C and pH 7.4. During incubation at 43 °C, neither Wt nor any of the mutant proteins exhibited light scattering, indicating that all proteins remained stable under conditions required for the CS aggregation assay. We found that R56A inhibited protein aggregation only marginally (∼9%) in the CS aggregation assay at a chaperone/substrate ratio of 1:3 (w/w) (parts B and D of Figure 2). However, at the same ratio, ΔR56 inhibited protein aggregation ∼30% more than the Wt (Figure 2D). We noted that the ΔA57 protein had a chaperone function similar to that of the Wt, but with ΔL55, it was slightly less (∼7%) than that of the Wt. We also compared the chaperone function of the Wt and mutant proteins by varying the ratio between α-crystallin and substrate proteins. In each case, we found that ΔR56 was superior to the Wt, while the three other mutants were either similar to or weaker than the Wt in preventing aggregation of a target protein (data not shown). Together, our findings indicate that substitution of alanine for arginine at position 56 results in a significant loss in chaperone function, whereas deletion of this arginine residue results in a paradoxical gain of chaperone function. To our knowledge, this is the first demonstration that deletion and substitution of the same amino acid residue has opposite effects on the chaperone function of αB-crystallin. Because deletion of L55 and A57 failed to improve the chaperone function (parts C and D of Figure 2), we can conclude that the improved chaperone function of αB-crystallin reported by Sharma and his colleagues (*38*) is likely due to the removal of the R56 residue.

At room temperature, α-crystallin has many hydrophobic pockets on its surface, as revealed by its binding to hydrophobic probes, such as ANS, bis-ANS, TNS, pyrene, etc. (*33*, *46*−*50*), while a number of reserve hydrophobic residues appear ready for relocation to the surface upon structural perturbation (*51*−*53*). Numerous studies showed a correlation between chaperone function and surface hydrophobicity in α-crystallin (*45*, *46*, *51*, *54*, *55*). We believe that exposure of additional hydrophobic sites at the surface underlies the improved chaperone activity of mutant proteins R21A and R103A of αA-crystallin compared to the Wt protein (*39*). Accordingly, we explored the relationship between enhanced chaperone activity in ΔR56 and the exposure of additional hydrophobic pockets using the hydrophobic probe, TNS. Figure 3 shows that, upon binding to the Wt, TNS displays intense fluorescence, with an emission maximum (λ_{max}) at 432 nm. This λ_{max} did not change in mutant proteins. However, the fluorescence intensity of ΔR56 was 68% more than that of the Wt. Fluorescence of ΔA57 increased only slightly (∼5%), but it decreased ∼21 and ∼33% in ΔL55 and R56A compared to the Wt protein (Figure 3). From data obtained with TNS, we established a decreasing order of surface hydrophobicity: ΔR56 > ΔA57 ≈ Wt > ΔL55 > R56A. Because these changes in surface hydrophobicity correspond to the order of decreasing chaperone function in these proteins, we

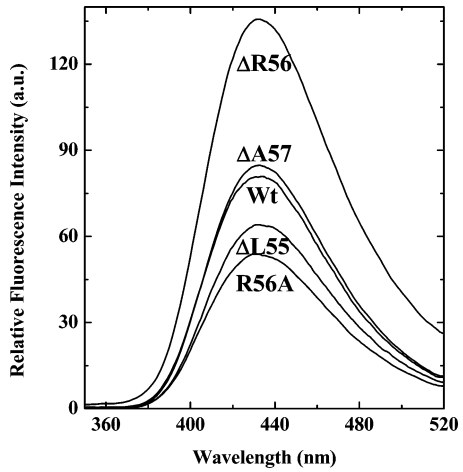

FIGURE 3: Fluorescence spectra of TNS-bound αB-crystallin. The fluorescence spectrum of different samples at 25 °C was recorded from 350 to 520 nm using an excitation wavelength of 320 nm. The protein concentration was 5 μM, and the TNS concentration was 100 μM.

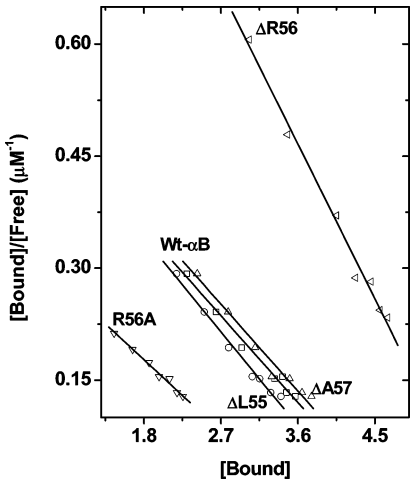

FIGURE 4: Binding parameters for the interaction between human αB-crystallin and CA at 57 °C. Scatchard plots for identical non-interacting multiple sites for calculating binding parameters.

conclude that the enhanced chaperone function of ΔR56 is due to increased surface hydrophobicity.

To determine how mutations affect the interaction between αB-crystallin and denaturing substrates, we measured the binding parameters using CA as the substrate. We incubated αB-crystallin (12.5 μM) for 1 h at 57 °C with various concentrations of CA (2−18 μM). Unbound (S) and bound CA were determined by filtration as described in the Experimental Procedures. Assuming an identical number of non-interacting sites per subunit of the chaperone, we determined the dissociation constant (K_d) by the Scatchard equation:

$$\tilde{\nu}/S = n/K_d - 1/K_d\tilde{\nu} \quad (2)$$

where $\tilde{\nu}$ is the number of moles of substrate bound per mole of chaperone, n is the number of binding sites, and K_d is the dissociation constant. The stoichiometry of n and K_d obtained from the plot of $\tilde{\nu}/S$ against $\tilde{\nu}$ (Figure 4) is 4.53 per subunit of αB-crystallin and 7.73 μM, respectively (Table 1). The number of CA-binding sites per subunit of αB-crystallin appears to be large. We found that the number of binding

Table 1: Determination of n and Dissociation Constant (K_d) for the Interaction of Different Human αB-Crystallins with CA at 57 °C

system studied	n	K_d (μM)
human αB-crystallin plus CA	4.53 ± 0.08	7.73 ± 0.42
ΔL55 plus CA	4.23 ± 0.07	7.14 ± 0.38
ΔR56 plus CA	5.62 ± 0.07	4.34 ± 0.20
ΔA57 plus CA	4.65 ± 0.12	7.73 ± 0.61
R56A plus CA	3.46 ± 0.08	9.38 ± 0.49

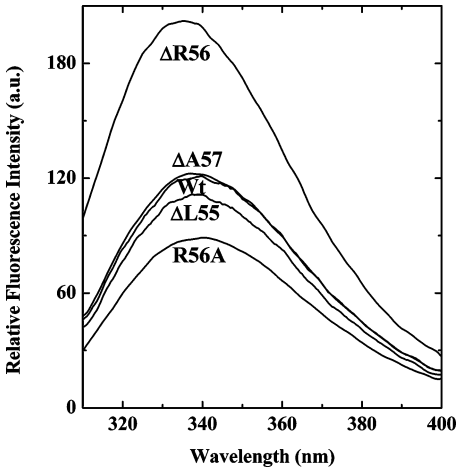

FIGURE 5: Intrinsic fluorescence spectra for the Wt and mutant αB-crystallins. The fluorescence spectrum of 0.1 mg/mL protein solutions was recorded from 310 to 400 nm at 25 °C using an excitation wavelength of 295 nm.

sites (n) per subunit of ΔR56 increased from 4.53 in the Wt to 5.62 and the association constant increased from 0.129 μM^{-1} (K_d = 7.73 μM) in the Wt to 0.230 μM^{-1} (K_d = 4.34 μM). In contrast, n for R56A decreased significantly from 4.53 to 3.46, and consequently, the association constant for this interaction decreased from 0.129 μM^{-1} (K_d = 7.73 μM) to 0.107 μM^{-1} (K_d = 9.38 μM). Deletion of L55 and A57 had no effect on the binding parameters for the interaction between Wt αB-crystallin and CA (Table 1). From these data, we conclude that the deletion of R56 of αB-crystallin increases its affinity for denatured proteins, whereas substitution of alanine for the charged arginine residue at position 56 dampens the interaction of αB-crystallin with the denatured substrate. In these experiments, we cannot rule out substrate−substrate aggregation/association before binding to αB-crystallin at 57 °C, which might give a higher number of n per molecule of αB-crystallin.

Our results demonstrate changes in the surface exposure of hydrophobic groups on the deletion mutant, ΔR56, and suggest that such changes affect the binding of substrate proteins under denaturating conditions, thus enhancing chaperone function. We used tryptophan fluorescence along with near- and far-UV CD techniques to determine whether these surface changes were accompanied by any change in the internal structure, such as perturbation in tertiary- and secondary-structural organization. Intrinsic fluorescence spectra indicated some differences between Wt and mutant proteins (Figure 5). While the fluorescence intensity of R56A decreased ~28% below that of the Wt, it increased dramatically in ΔR56 (~65%). We also observed alterations in fluorescence emission maxima for these two mutants. The fluorescence emission maximum (λ_{max}) of Wt αB-crystallin was at 337 nm. We found that the λ_{max} of the ΔR56 mutant

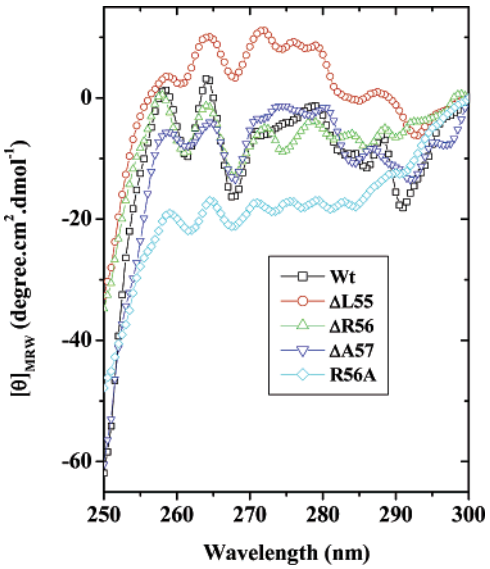

FIGURE 6: Near-UV CD spectra of the Wt and mutant αB-crystallins. Spectra were collected at a 0.5 nm wavelength interval using a 10 mm path-length CD cell. The protein concentration was 1.0 mg/mL.

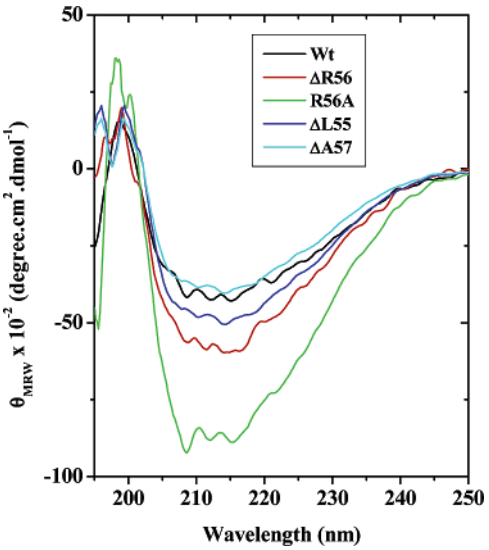

FIGURE 7: Far-UV CD spectra of recombinant αB-crystallin. Spectra were recorded for 0.2 mg/mL protein (in 10 mM phosphate buffer at pH 7.2) using a 1.0 mm path-length cell. The data interval is 0.2 nm.

exhibited ~2 nm blue shift (335 nm), whereas that emission maxima for R56A mutant was at 340 nm, i.e., ~3 nm red shift. The λ_{max} values for ΔL55 and ΔA57 were 338.5 and 339.5 nm, i.e., ~1.5 and 2.5 nm red shift, respectively. The changes in fluorescence intensity and λ_{max} may reflect changes in the microenvironment of Trp^{60}, which is located close to the mutation sites of the protein.

Near-UV CD spectra of Wt and mutant αB-crystallins support our intrinsic fluorescence data (Figure 6). The near-UV CD spectrum of the Wt had five distinct maxima and five distinct minima, which is quite similar to previously published results (*56*). The negative vibronic signals at ~291 and ~285 nm (minima) are from tryptophan residues. The maxima close to 260 and 265 nm and the minima close to 268 and 261 nm indicate a phenylalnine fine structure. The remaining transitions between 270 and 290 nm arise from tyrosine and/or tryptophan. The signal for phenylalanine in the 250−270 nm region was minimally altered in all mutants compared to the Wt protein, although the intensity values decreased sharply for R56A. Beyond 270 nm, the spectral characteristics of this mutant protein differed both in intensity and position from those for the Wt protein. As expected, we noticed spectral shifts in the other mutants as well. ΔR56 showed a slight alteration in the peak position beyond 270 nm, and deletion of L55 and A57 shifted the near-UV CD spectra both in intensity and position (beyond 270 nm). Because these residues are close to Trp^{60}, we assume that these deletions alter the microenvironments of tyrosine and/or tryptophan in αB-crystallin.

Mutation of R56 perturbed not only the tertiary structure of αB-crystallin but also its secondary structure, as indicated by far-UV CD spectra (Figure 7). The spectra were quantitatively analyzed using CONTINLL (*41*) The estimated levels of secondary structure are listed in Table 2. We estimated ~32% *β*-sheet and ~15% α-helix content, which corresponds to published estimates of the secondary structure for αB-crystallin (*46*, *57*). For R56A, the α-helix content increased from 15 to 29% and the *β*-sheet content decreased from 32 to 18%. Deletion of R56 caused minimal alterations

Table 2: Different Secondary-Structural Elements in Wt αB-Crystallin and Its Mutants Using CONTINLL Software

proteins	α helix	*β* sheet	*β* turn	random coil
Wt	14.8	31.8	22.6	30.8
ΔL55	17.6	28.9	23.0	30.5
ΔR56	20.4	26.9	23.1	29.6
ΔA57	14.4	32.1	22.9	30.6
R56A	29.2	17.9	22.6	30.3

Table 3: Oligomeric Size of the Wt and Mutant Human αB-Crystallin Determined by Dynamic Light Scattering

proteins	M_w (g/mol)	PDI	R_h (nm)
Wt	$7.93 \pm 0.01 \times 10^5$	1.010 (0.3%)	8.2 ± 0.2
ΔL55	$7.45 \pm 0.02 \times 10^5$	1.017 (0.3%)	8.4 ± 0.2
ΔR56	$9.71 \pm 0.01 \times 10^5$	1.010 (0.5%)	8.1 ± 0.2
ΔA57	$7.72 \pm 0.02 \times 10^5$	1.001 (0.4%)	8.4 ± 0.2
R56A	$7.47 \pm 0.01 \times 10^5$	1.007 (0.3%)	8.4 ± 0.2

of the secondary structure (Table 2). Therefore, we can conclude that deletion and substitution of R56 have opposing effects on the structural integrity of αB-crystallin.

Dynamic light scattering (multi-angle light scattering coupled with size-exclusion chromatography) determines polydispersity and estimates the absolute molar mass and size of proteins. We used this technique to determine whether the perturbation in secondary and tertiary structures altered the quaternary structure, i.e., oligomeric size, of αB-crystallin. Wt and mutant proteins (except R56A) had slightly different elution profiles (Figure 8). However, from data in Table 3, it is evident that perturbation in secondary and tertiary structures had little effect on the molecular mass. Even polydispersity and hydrodynamic radii (R_h) remained unaltered (Table 3). Overall, these findings suggest that residues 55−57 of αB-crystallin do not affect the homo-oligomerization of the protein. Shreelakshmi et al. (*28*) reported earlier that R50 and P51 residues in "substrate recognition sequence 1" ($_{42}$TSLSPFYLRPPSFLRA$_{57}$) had no effect on the oligomeric size of αB-crystallin. Our results confirm these findings, and we believe that the peptide sequence, $_{50}$RPPSFLRA$_{57}$, is not essential for protein oligomerization.

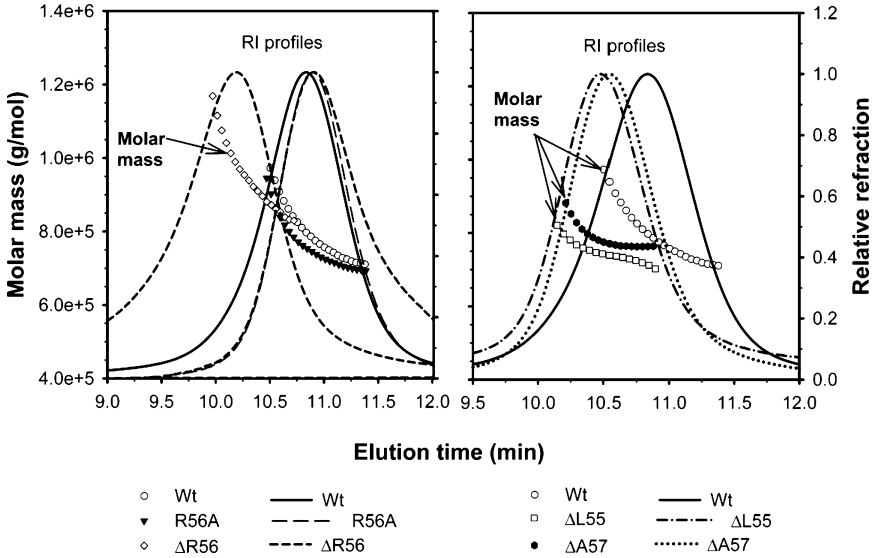

FIGURE 8: Elution profiles of the Wt and mutant αB-crystallins. Molar mass distribution across refractive index peaks of the Wt, R56A, and ΔR56 (A) and the Wt, ΔL55, and ΔA57 (B) determined by dynamic light scattering measurements. Data acquired from RI and DAWN-QELS detectors were analyzed using ASTRA (5.1.5) software developed by Wyatt Technologies, Santa Barbara, CA.

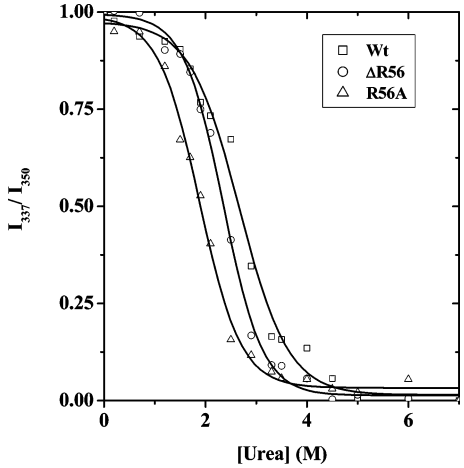

FIGURE 9: Thermodynamic stability of human αB-crystallin. Equilibrium urea unfolding profile for 0.1 mg/mL Wt and mutant αB-crystallins at 25 °C. The profile is normalized to a scale of 0−1. Symbols represent the experimental data points, and the solid lines represent the best fit according to the three-state model described by eq 3.

Although there is a general belief that exposed surface hydrophobic sites are responsible for chaperone function of α-crystallin (*45*, *46*, *51*, *54*, *55*), recent studies imply that other factors, such as oligomerization, structural perturbation, and subunit interaction, may also be responsible (*33*, *36*, *49*, *51*−*53*, *58*−*61*). To quantify the structural perturbation because of R56 mutations, we compared the thermodynamic stability of Wt and mutant αB-crystallins. We measured equilibrium urea unfolding by following tryptophan fluorescence of the proteins at various urea concentrations. Native and unfolded αB-crystallins have λ_{max} values of 337 and 350 nm. We plotted the ratio of intensities at 337 and 350 nm as a function of the urea concentration and generated sigmoidal curves for all three proteins (Figure 9). A rough estimate of the transition midpoint ($C_{1/2}$) of Wt αB-crystallin indicated $C_{1/2}$ at 2.6 M urea. $C_{1/2}$ decreased marginally (2.4 M) for the ΔR56 mutant but decreased further (1.8 M) for the R56A mutant. The reduction in thermodynamic stability indicates that substitution of arginine 56 by alanine causes important structural perturbations of αB-crystallin.

It can be seen that the profiles lack strong cooperativity, indicating multistate transitions. Sun et al. (*62*). analyzed the unfolding profile of recombinant αB-crystallin by the three-state model according to the native ⇆ intermediate ⇆ unfolded scheme. The present profiles of Wt and mutant αB-crystallins were fitted to the three-state model (*42*, *45*, *62*) according to the following equation:

$$I = \frac{I_o + I_1\exp(-\Delta G_1^0 + m_1[\text{urea}])/RT + I_\infty\exp(-\Delta G_2^0 + m_2[\text{urea}])/RT}{1 + \exp(-\Delta G_1^0 + m_1[\text{urea}])/RT + \exp(-\Delta G_2^0 + m_2[\text{urea}])/RT} \quad (3)$$

where I_o, I_1, and I_∞ are the signal intensities for the 100% native, 100% intermediate, and 100% unfolded forms, respectively. ΔG_1^0 refers to the standard free-energy change between the native and intermediate forms, and ΔG_2^0 refers to the standard free-energy change between the intermediate and unfolded forms. ΔG^0, being the sum of ΔG_1^0 and ΔG_2^0, refers to the standard free-energy change of unfolding (between native and unfolded forms) at the urea concentration of 0. Table 4 lists the fitted parameters. The standard free-energy change of αB-crystallin unfolding at 25 °C is 22.51 kJ/mol. This value of ΔG^0 is comparable to that reported by Sun et al. (*62*) from guanidine hydrochloride unfolding (21.0 kJ/mol). Deletion of R56 lowered the thermodynamic stability by approximately 5 kJ/mol. The ΔG^0 value for R56A decreased to 12.76 kJ/mol, indicating a reduction in thermodynamic stability (ΔG^0) of ∼10 kJ/mol.

There are differing views as to the role of the peptide $_{43}$SLSPFYLRPPSFLRAPSWF$_{61}$ in the chaperone function and αA−αB subunit interaction. Whereas Sreelakshmi et al. (*28*) reported that a peptide within this sequence binds to αA-crystallin and the binding does not affect the chaperone function, Ghosh et al. (*30*) reported that the $_{43}$SLSPFYLRPPSFLRAP$_{58}$ sequence in αB-crystallin has a dual role, in both subunit interaction with αA-crystallin and chaperone function. Our findings indicate that mutation in this region influences the chaperone function of αB-crystallin (Figure 2). Additionally, we confirmed the importance of the arginine mutation within this peptide sequence for subunit exchange

Table 4: Parameters of Equilibrium Urea Unfolding of Human αB-Crystallin and Its Mutants at 25 °C, Obtained from the Three-State Model (N ↔ I ↔ U) Fit

systems studied	ΔG_1^0 (kJ mol^{-1})	ΔG_2^0 (kJ mol^{-1})	ΔG^0 (kJ mol^{-1})	m_1 (kJ mol^{-1} M^{-1})	m_2 (kJ mol^{-1} M^{-1})
human αB	6.30 ± 0.32	16.21 ± 0.54	22.51 ± 0.43	5.97 ± 0.55	7.49 ± 0.81
ΔR56	4.52 ± 0.51	13.01 ± 0.68	17.53 ± 0.60	6.11 ± 0.51	7.61 ± 0.73
R56A	2.31 ± 0.67	10.45 ± 0.46	12.76 ± 0.57	4.88 ± 0.31	7.11 ± 0.52

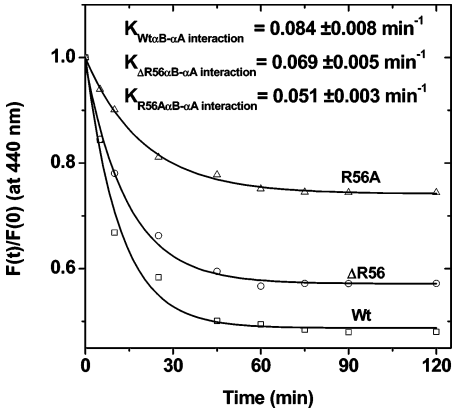

FIGURE 10: Subunit exchange of the Wt and mutant αB-crystallins with αA-crystallin. Decrease in fluorescence intensity at 440 nm as a function of time. A total of 25 μg of Alexa fluor 350-labeled Wt or mutant αB-crystallin and 75 μg of Alexa fluor 488-labeled αA-crystallin were mixed at 37 °C. The fluorescence spectrum (400−600 nm) was taken at various intervals from samples at room temperature (25 °C). The excitation wavelength was 346 nm. The curves were fitted according to eq 1.

with αA-crystallin by the FRET assay (because deletion of L55 and A57 do not affect the structure and chaperone function of αB-crystallin, we excluded them from this particular experiment). As expected, we observed a time-dependent decrease in Alexa fluor 350 emission intensity at 440 nm and a concomitant increase in Alexa fluor 488 fluorescence intensity at 520 nm. The reaction was completed by 2 h at 37 °C (Figure 10). The subunit exchange rate constant (k) was then derived by fitting the declining Alexa fluor 350 intensity to eq l: $F(t)/F(0) = A + Be^{-kt}$. From this method, we calculated the k value for the Wt to be 0.084 min^{-1}, which agrees with previously reported values (*28*, *60*, *63*). Rate constants for ΔR56 and R56A were 0.069 and 0.051 min^{-1}, respectively Thus, deletion of R56 reduced the subunit exchange rate by ∼18%, and the substitution of alanine for arginine reduced it further (∼39%). Our findings indicate that R56 is critical within this peptide sequence ($_{43}$-SLSPFYLRPPSFLRAP$_{58}$), for subunit interaction with αA-crystallin.

The correlation between subunit interaction and chaperone function of α-crystallin is still unclear. Several previous studies showed that an increase in αA−αB subunit interaction enhances the chaperone function (*49*, *60*, *61*), whereas others suggest that subunit interactions do not influence chaperone function (*28*, *34*, *40*, *63*). Our own studies failed to indicate a correlation between the subunit interaction and chaperone function of αB-crystallin. We speculate that subunit exchange in α-crystallin may be required to attain an optimum ratio of αA and αB that confers a stable conformation to the oligomeric assembly of the protein.

We find that deletion of R56 causes subtle structural perturbations that result in exposed hydrophobic surfaces and enhanced chaperone-like function. These findings are consistent with previously published results relating the structural perturbation of α-crystallin to enhanced chaperone function (*51*−*53*, *58*, *59*). We find that the R56A mutation perturbs the αB-crystallin structure more than ΔR56 and decreases surface hydrophobicity and chaperone function. We speculate that, in addition to surface hydrophobicity, subunit exchange, and oligomeric structure, the positive charge on selected arginine residues is also likely to influence the chaperone function of αB-crystallin, similar to our findings with αA-crystallin (*39*).

ACKNOWLEDGMENT

The authors thank Michael Zagorski and Krzysztof Palczewski of Case Western Reserve University, Cleveland, OH, for use of the CD spectropolarimeter and the fluorescence spectrofluorometer.

REFERENCES

1. de Jong, W. W. (1981) Evolution of lens and cystallins, in *Molecular and Cellular Biology of the Eye Lens*, pp 221−278, Wiley, New York.
2. Narberhaus, F. (2002) α-Crystallin-type heat shock proteins: Socializing minichaperones in the context of a multichaperone network, *Microbiol. Mol. Biol. Rev. 66*, 64−93.
3. Bloemendal, H., and de Jong, W. W. (1991) Lens proteins and their genes, *Prog. Nucleic Acid. Res. Mol. Biol. 41*, 259−281.
4. Piatigorsky, J. (1992) Lens crystallins. Innovation associated with changes in gene regulation, *J. Biol. Chem. 267*, 4277−4280.
5. Wistow, G. J., and Piatigorsky, J. (1988) Lens crystallins: The evolution and expression of proteins for a highly specialized tissue, *Annu. Rev. Biochem. 57*, 479−504.
6. Mandal, K., Dillon, J., and Gaillard, E. R. (2000) Heat and concentration effects on the small heat shock protein, α-crystallin, *Photochem. Photobiol. 71*, 470−475.
7. Duncan, M. K., Cvekl, A., Kantorow, M., and Piatigorsky, J. (2004) Lens Crystallins, in *Development of the Ocular Lens* (Lovicu, F. J., and Robinson, M. L., Eds.) pp 119−150, Cambridge University Press, Cambridge, U.K.
8. Ingolia, T. D., and Craig, E. A. (1982) Four small *Drosophila* heat shock proteins are related to each other and to mammalian α-crystallin, *Proc. Natl. Acad. Sci. U.S.A. 79*, 2360−2364.
9. Groenen, P. J., Merck, K. B., de Jong, W. W., and Bloemendal, H. (1994) Structure and modifications of the junior chaperone α-crystallin. From lens transparency to molecular pathology, *Eur. J. Biochem. 225*, 1−19.
10. Sax, C. M., and Piatigorsky, J. (1994) Expression of the α-crystallin/small heat-shock protein/molecular chaperone genes in the lens and other tissues, *Adv. Enzymol. Relat. Areas Mol. Biol. 69*, 155−201.
11. Klemenz, R., Frohli, E., Steiger, R. H., Schafer, R., and Aoyama, A. (1991) αB-Crystallin is a small heat shock protein, *Proc. Natl. Acad. Sci. U.S.A. 88*, 3652−3656.
12. Srinivasan, A. N., Nagineni, C. N., and Bhat, S. P. (1992) αA-Crystallin is expressed in non-ocular tissues, *J. Biol. Chem. 267*, 23337−23341.
13. Bhat, S. P., and Nagineni, C. N. (1989) αB subunit of lens-specific protein α-crystallin is present in other ocular and non-ocular tissues, *Biochem. Biophys. Res. Commun. 158*, 319−325.
14. Deretic, D., Aebersold, R. H., Morrison, H. D., and Papermaster, D. S. (1994) αA- and αB-crystallin in the retina. Association with the post-Golgi compartment of frog retinal photoreceptors, *J. Biol. Chem. 269*, 16853−16861.

15. Kato, K., Shinohara, H., Kurobe, N., Goto, S., Inaguma, Y., and Ohshima, K. (1991) Immunoreactive αA-crystallin in rat non-lenticular tissues detected with a sensitive immunoassay method, *Biochim. Biophys. Acta 1080*, 173−180.
16. Horwitz, J. (1992) α-Crystallin can function as a molecular chaperone, *Proc. Natl. Acad. Sci. U.S.A. 89*, 10449−10453.
17. Kim, K. K., Kim, R., and Kim, S. H. (1998) Crystal structure of a small heat-shock protein, *Nature 394*, 595−599.
18. van Montfort, R. L., Basha, E., Friedrich, K. L., Slingsby, C., and Vierling, E. (2001) Crystal structure and assembly of a eukaryotic small heat shock protein, *Nat. Struct. Biol. 8*, 1025−1030.
19. de Jong, W. W., Caspers, G. J., and Leunissen, J. A. (1998) Genealogy of the α-crystallin small heat-shock protein superfamily, *Int. J. Biol. Macromol. 22*, 151−162.
20. Smulders, R., Carver, J. A., Lindner, R. A., van Boekel, M. A., Bloemendal, H., and de Jong, W. W. (1996) Immobilization of the C-terminal extension of bovine αA-crystallin reduces chaperone-like activity, *J. Biol. Chem. 271*, 29060−29066.
21. Thampi, P., and Abraham, E. C. (2003) Influence of the C-terminal residues on oligomerization of αA-crystallin, *Biochemistry 42*, 11857−11863.
22. Pasta, S. Y., Raman, B., Ramakrishna, T., and Rao, Ch. M. (2002) Role of the C-terminal extensions of α-crystallins. Swapping the C-terminal extension of α-crystallin to αB-crystallin results in enhanced chaperone activity, *J. Biol. Chem. 277*, 45821−45828.
23. Liu, C., and Welsh, M. J. (1999) Identification of a site of Hsp27 binding with Hsp27 and αB-crystallin as indicated by the yeast two-hybrid system, *Biochem. Biophys. Res. Commun. 255*, 256−261.
24. Fu, L., and Liang, J. J. (2002) Detection of protein−protein interactions among lens crystallins in a mammalian two-hybrid system assay, *J. Biol. Chem. 277*, 4255−4260.
25. Fu, L., and Liang, J. J. (2003) Alteration of protein−protein interactions of congenital cataract crystallin mutants, *Invest. Ophthalmol. Vis. Sci. 44*, 1155−1159.
26. Merck, K. B., De Haard-Hoekman, W. A., Oude, Essink, B. B., Bloemendal, H., and de Jong, W. W. (1992) Expression and aggregation of recombinant αA-crystallin and its two domains, *Biochim. Biophys. Acta 1130*, 267−276.
27. Pasta, S. Y., Raman, B., Ramakrishna, T., and Rao Ch. M. (2003) Role of the conserved SRLFDQFFG region of α-crystallin, a small heat shock protein. Effect on oligomeric size, subunit exchange, and chaperone-like activity, *J. Biol. Chem. 278*, 51159−51166.
28. Sreelakshmi, Y., Santhoshkumar, P., Bhattacharyya, J., and Sharma, K. K. (2004) αA-Crystallin interacting regions in the small heat shock protein, αB-crystallin, *Biochemistry 43*, 15785−15795.
29. Ghosh, J. G., and Clark, J. I. (2005) Insights into the domains required for dimerization and assembly of human αB crystallin, *Protein Sci. 14*, 684−695.
30. Ghosh, J. G., Estrada, M. R., and Clark, J. I. (2005) Interactive domains for chaperone activity in the small heat shock protein, human αB crystallin, *Biochemistry 44*, 14854−14869.
31. Shroff, N. P., Cherian-Shaw, M., Bera, S., and Abraham, E. C. (2000) Mutation of R116C results in highly oligomerized αA-crystallin with modified structure and defective chaperone-like function, *Biochemistry 39*, 1420−1426.
32. Kumar, L. V., Ramakrishna, T., and Rao, C. M. (1999) Structural and functional consequences of the mutation of a conserved arginine residue in αA and αB crystallins, *J. Biol. Chem. 274*, 24137−24141.
33. Bera, S., Thampi, P., Cho, W. J., and Abraham, E. C. (2002) A positive charge preservation at position 116 of αA-crystallin is critical for its structural and functional integrity, *Biochemistry 41*, 12421−12426.
34. Bera, S., and Abraham, E. C. (2002) The αA-crystallin R116C mutant has a higher affinity for forming heteroaggregates with αB-crystallin, *Biochemistry 41*, 297−305.
35. Cobb, B. A., and Petrash, J. M. (2000) Structural and functional changes in the αA-crystallin R116C mutant in hereditary cataracts, *Biochemistry 39*, 15791−15798.
36. Bova, M. P., Yaron, O., Huang, Q., Ding, L., Haley, D. A., Stewart, P. L., and Horwitz, J. (1999) Mutation R120G in αB-crystallin, which is linked to a desmin-related myopathy, results in an irregular structure and defective chaperone-like function, *Proc. Natl. Acad. Sci. U.S.A. 96*, 6137−6142.
37. Nagaraj, R. H., Oya-Ito, T., Padayatti, P. S., Kumar, R., Mehta, S., West, K., Levison, B., Sun, J., Crabb, J. W., and Padival, A. K. (2003) Enhancement of chaperone function of α-crystallin by methylglyoxal modification, *Biochemistry 42*, 10746−10755.
38. Sharma, K. K., and Santhoshkumar, P. (2005) Deletion of residues 54−61 (FLRAPSWF) in αB-crystallin leads to decreased oligomeric mass with increased chaperone-like activity, *Invest. Ophthalmol. Vis. Sci. 46*, Abstract 3486.
39. Biswas, A., Miller, A., Oya-Ito, T., Santhoshkumar, P., Bhat, M., and Nagaraj, R. H. (2006) Effect of site-directed mutagenesis of methylglyoxal-modifiable arginine residues on the structure and chaperone function of human αA-crystallin, *Biochemistry 45*, 4569−4577.
40. Sreelakshmi, Y., and Sharma, K. K. (2005) Recognition sequence 2 (residues 60−71) plays a role in oligomerization and exchange dynamics of αB-crystallin, *Biochemistry 44*, 12245−12252.
41. Provencher, S. W., and Glockner, J. (1981) Estimation of globular protein secondary structure from circular dichroism, *Biochemistry 20*, 33−37.
42. Das, B. K., Bhattacharyya, T., and Roy, S. (1995) Characterization of a urea induced molten globule intermediate state of glutaminyl-tRNA synthetase from *Escherichia coli*, *Biochemistry 34*, 5242−5247.
43. Bhattacharyya, J., and Das, K. P. (1998) α-Crystallin does not require temperature activation for its chaperone-like activity, *Biochem. Mol. Biol. Int. 46*, 249−258.
44. Santhoshkumar, P., and Sharma, K. K. (2001) Phe71 is essential for chaperone-like function in αA-crystallin, *J. Biol. Chem. 276*, 47094−47099.
45. Biswas, A., and Das, K. P. (2004) Role of ATP on the interaction of α-crystallin with its substrates and its implications for the molecular chaperone function, *J. Biol. Chem. 279*, 42648−42657.
46. Reddy, G. B., Das, K. P., Petrash, J. M., and Surewicz, W. K. (2000) Temperature-dependent chaperone activity and structural properties of human αA- and αB-crystallins, *J. Biol. Chem. 275*, 4565−4570.
47. Kumar, M. S., Kapoor, M., Sinha, S., and Reddy, G. B. (2005) Insights into hydrophobicity and the chaperone-like function of αA- and αB-crystallins: An isothermal titration calorimetric study, *J. Biol. Chem. 280*, 21726−21730.
48. Shroff, N. P., Bera, S., Cherian-Shaw, M., and Abraham, E. C. (2001) Substituted hydrophobic and hydrophilic residues at methionine-68 influence the chaperone-like function of αB-crystallin, *Mol. Cell. Biochem. 220*, 127−133.
49. Gupta, R., and Srivastava, O. P. (2004) Deamidation affects structural and functional properties of human αA-crystallin and its oligomerization with αB-crystallin, *J. Biol. Chem. 279*, 44258−44269.
50. Raman, B., and Rao, C. M. (1994) Chaperone-like activity and quaternary structure of α-crystallin, *J. Biol. Chem. 269*, 27264−27268.
51. Das, K. P., and Surewicz, W. K. (1995) Temperature-induced exposure of hydrophobic surfaces and its effect on the chaperone activity of α-crystallin, *FEBS Lett. 369*, 321−325.
52. Smith, J. B., Liu, Y., and Smith, D. L. (1996) Identification of possible regions of chaperone activity in lens α-crystallin, *Exp. Eye Res. 63*, 125−128.
53. Rao, C. M., Raman, B., Ramakrishna, T., Rajaraman, K., Ghosh, D., Datta, S., Trivedi, V. D., and Sukhaswami, M. B. (1998) Structural perturbation of α-crystallin and its chaperone-like activity, *Int. J. Biol. Macromol. 22*, 271−281.
54. Saha, S., and Das, K. P. (2004) Relationship between chaperone activity and oligomeric size of recombinant human αA- and αB-crystallin: A tryptic digestion study, *Proteins 57*, 610−617.
55. Raman, B., Ramakrishna, T., and Rao, C. M. (1995) Temperature dependent chaperone-like activity of α-crystallin, *FEBS Lett. 365*, 133−136.
56. Sun, T. X., Das, B. K., and Liang, J. J. (1997) Conformational and functional differences between recombinant human lens αA- and αB-crystallin, *J. Biol. Chem. 272*, 6220−6225.
57. Biswas, A., and Das, K. P. (2004) SDS induced structural changes in α-crystallin and its effect on refolding, *Protein J. 23*, 529−538.
58. Palmisano, D. V., Groth-Vasselli, B., Farnsworth, P. N., and Reddy, M. C. (1995) Interaction of ATP and lens α crystallin characterized by equilibrium binding studies and intrinsic tryptophan fluorescence spectroscopy, *Biochim. Biophys. Acta 1246*, 91−97.

59. Borkman, R. F., Knight, G., and Obi, B. (1996) The molecular chaperone α-crystallin inhibits UV-induced protein aggregation, *Exp. Eye Res. 62*, 141−148.
60. Bova, M. P., Ding, L. L., Horwitz, J., and Fung, B. K. (1997) Subunit exchange of αA-crystallin, *J. Biol. Chem. 272*, 29511−29517.
61. Srinivas, V., Raman, B., Rao, K. S., Ramakrishna, T., and Rao, Ch. M. (2005) Arginine hydrochloride enhances the dynamics of subunit assembly and the chaperone-like activity of α-crystallin, *Mol. Vis. 11*, 249−255.
62. Sun, T. X., Akhtar, N. J., and Liang, J. J. (1999) Thermodynamic stability of human lens recombinant αA- and αB-crystallins, *J. Biol. Chem. 274*, 34067−34071.
63. Aquilina, J. A., Benesch, J. L., Ding, L. L., Yaron, O., Horwitz, J., and Robinson, C. V. (2005) Subunit exchange of polydisperse proteins: Mass spectrometry reveals consequences of αA-crystallin truncation, *J. Biol. Chem. 280*, 14485−14491.

BI061323W